land

MDPI

Article

Spatial Expansion Characteristics and Nonlinear Relationships of Driving Factors in Urban Agglomerations: A Case Study of the Yangtze River Delta Urban Agglomeration in China

Bochuan Zhao [1,†], Yifei Wang [2,†], Huizhi Geng [1,*], Xuan Jiang [1] and Lingyue Li [1]

[1] College of Architecture and Urban Planning, Tongji University, Shanghai 200092, China; zbccqsh@tongji.edu.cn (B.Z.); jiangxuansn@163.com (X.J.); lilingyue@tongji.edu.cn (L.L.)
[2] Department of Geography and Geoinformation Science, George Mason University, Fairfax, VA 22030, USA; ywang214@gmu.edu
* Correspondence: genghuizhi@163.com
† These authors contributed equally to this work.

Abstract: Urban agglomerations are increasingly becoming the primary regional units in global competition, characterized by the rapid expansion of impervious surface areas, which negatively impacts both society and the environment. This study quantifies the spatiotemporal expansion of these surfaces in the Yangtze River Delta urban agglomeration and explores its driving factors using a Geographically Weighted Random Forest model. The results demonstrate a transition from "point expansion" to "infill development", while also revealing a gradual southward shift in the developmental focus of the Yangtze River Delta urban agglomeration. Although expansion intensity has decreased, spatial clustering has intensified. Based on the expansion patterns of impervious surface areas, we propose a novel regional classification method, dividing the Yangtze River Delta urban agglomeration into three zones: "A-Development Decline Zone", "B-Development Core Zone", and "C-Development Ascendance Zone". Socio-economic factors are the primary drivers of this expansion, followed by science and education, and then the ecological environment, while physical geography factors have the least impact. The study reveals differentiated regional development characteristics and further refines the sub-regions within the urban agglomeration, providing a new perspective for future regional coordinated development policies.

Keywords: impervious surface areas; spatial expansion; regional development zones; geographically weighted random forest; urban agglomeration

Citation: Zhao, B.; Wang, Y.; Geng, H.; Jiang, X.; Li, L. Spatial Expansion Characteristics and Nonlinear Relationships of Driving Factors in Urban Agglomerations: A Case Study of the Yangtze River Delta Urban Agglomeration in China. *Land* **2024**, *13*, 1951. https://doi.org/10.3390/land13111951

Academic Editor: Chuanrong Zhang

Received: 17 October 2024
Revised: 9 November 2024
Accepted: 13 November 2024
Published: 19 November 2024

1. Introduction

With the continuous progression of global urbanization, special urbanization phenomena such as urban agglomerations, mega-cities, and metropolitan areas have gradually emerged. Among these, the spatial expansion of city clusters has become a focal point of widespread attention, gradually replacing individual cities as the primary regional units for global competition and specialization [1]. A prominent feature of urban agglomerations' spatial expansion is the increase in impervious surface areas (ISAs), such as asphalt roads, houses, and parking lots, which are artificially constructed rather than naturally formed and block water from seeping into the ground. The uncontrolled increase in ISAs places significant pressure on the regional ecological environment [2]. In recent years, global ISA datasets derived from long-term, multi-temporal remote sensing data have played an increasingly crucial role in studying urban spatial morphology [3]. The Yangtze River Delta Urban Agglomeration (YRDUA) stands out as one of China's most robustly urbanized regions, making its spatial expansion characteristics highly typical [4]. The YRDUA's significance extends far beyond its role as an urbanized region. As China's largest and

most dynamic urban agglomeration, it is a crucial engine for national economic development, contributing approximately 24.3% to China's GDP and housing over 235 million residents [5]. The region's unique geographical characteristics, featuring a dense water network (3–4 km/km^2) and predominantly flat terrain (60% plains), have historically provided favorable conditions for urban development while presenting ecological challenges [6]. These environmental and cultural factors and its rapid economic growth have made the YRDUA an ideal case for studying complex urban expansion processes. Therefore, analyzing the spatiotemporal characteristics of ISA expansion in the YRDUA and identifying its driving factors is of significant guiding importance for the sustainable development of the regional economy and society as well as ecological and environmental protection.

The study of ISAs originated in the field of remote sensing, and early scholars focused on the identification and extraction of ISAs [7]. With the rapid development of artificial intelligence, methods such as Decision Trees [8], Attention Transfer Mechanisms [9], Random Forests [10], and Neural Networks [11,12] have been increasingly applied to ISA dataset generation, significantly improving recognition accuracy and speed. Concurrently, research on ISAs has gradually begun to integrate with studies on urban heat island effects and urban hydrology. These studies primarily explore the relationship between ISAs and urban surface temperatures [3], and ISAs' impact on surface rivers [13]. With the improved availability and identification accuracy of ISA datasets, scholars have begun to explore the relationship between ISAs and urban spatial morphology. Numerous studies have shown that changes in ISAs effectively reflect the spatial pattern evolution of urban expansion [14]. Researchers have revealed the spatial and temporal change characteristics of ISAs using methods such as Center of Gravity Analysis [15], the Dilatancy Index [16], the Landscape Pattern Index [17], Standard Ellipse Difference [18], and the Moran Index [19]. These methods effectively describe the spatial distribution characteristics of ISAs, using indicators such as patch density and fractal dimension to reveal their spatial patterns. However, these methods seldom focus on the spatial clustering characteristics of ISAs, limiting our comprehensive understanding of expansion patterns. Additionally, some scholars have primarily explored the evolutionary patterns of ISAs at the city scale. Li et al. used TM imagery to analyze the characteristics of ISA expansion in Harbin [20]. Other scholars have used similar methods to study the expansion of ISAs in cities such as Shanghai [21], Guangzhou [22], and Xiamen [23]. Lu, Guan, and He used the urban expansion index to study land expansion in the Wuhan urban agglomeration [24]. Ma, Wu, and Wang analyzed the changing relationship between ISAs, spatial stratification, and population in three major urban agglomerations in China [25]. In the case of the YRDUA, scholars have focused more on the expansion characteristics of its construction land [26]. Comparatively, more research is needed on ISA expansion at the urban agglomeration scale. Since urban agglomerations serve as crucial spatial entities for regional development, the lack of research scale may impact our understanding of ISA expansion characteristics at the regional level.

As research has progressed, scholars have increasingly focused on the factors influencing ISA expansion. Linear regression models are widely used in this field. For instance, Zhou, Chen, and Li employed regression models to analyze the driving factors behind the landscape pattern changes of ISAs in Xiamen [23]. Gao, Li, and Wang (2023) quantified the driving factors of ISA expansion in Shanghai through integrated correlation analysis and generalized additive models [21]. Zhao, Li, Wang, and Zhang (2023) applied the Mann–Kendall Trend Test method to quantitatively analyze ISA change characteristics and then used the Geographical Detector Model to analyze the driving factors behind ISA expansion in the Central Plains urban agglomeration [15]. The relationship between ISA expansion and its drivers is intricate and not always straightforward or linear [27,28]. To address this issue, Wu, Li, Zhang, and Liu used Boosted Regression Tree models to analyze the main drivers of ISA changes in Shenyang from 2010 to 2017 [29]. However, natural and socio-economic factors are not evenly distributed in space, which makes spatial heterogeneity an important issue [28], which was overlooked in the research above. To address spatial heterogeneity, Wu, Yang, Yin, and Zhang used Geographically Weighted

Regression (GWR) based on ISA data to analyze the characteristics of urban land expansion in 41 Chinese cities [30].

Although significant progress has been made in understanding ISA expansion's characteristics and driving factors, several areas for improvement still need to be addressed. Firstly, current research methods lack sufficient spatial clustering analysis, resulting in an incomplete understanding of the spatial distribution characteristics of ISAs. Secondly, research often focuses on prefecture-level cities rather than urban agglomerations, resulting in a limited understanding of expansion characteristics and their impact mechanisms at larger scales. Furthermore, existing studies have failed to simultaneously address the nonlinear relationships between driving factors and spatial heterogeneity; thus, they have been unable to reveal the complex interactions among various factors fully. To ensure accurate analysis results, both the nonlinear relationships in the model and the impact of spatial heterogeneity should be comprehensively considered. Existing Random Forest Models excel at capturing nonlinear relationships among variables but struggle with spatial heterogeneity [18,31]. Conversely, GWR models fully consider spatial heterogeneity but find it challenging to handle nonlinear relationships [32]. Therefore, this study introduces the Geographically Weighted Random Forest (GWRF) model to identify the driving factors of ISA expansion in the YRDUA. This locally nonlinear spatial machine learning method effectively handles the high-dimensional nonlinear relationships among variables and the spatial heterogeneity characterized by the significance of the explanatory variables [33,34].

Coordinated regional development is key to achieving high-quality growth. An in-depth analysis of ISA expansion characteristics in urban agglomerations and their driving factors is crucial for maintaining regional ecosystem balance and optimizing territorial spatial development patterns. Therefore, the research objectives of this study are as follows: ① To systematically characterize the spatiotemporal expansion patterns of ISAs in the YRDUA from 2000 to 2020, revealing overall growth trends. ② To analyze the spatial clustering characteristics of ISA expansion and its evolutionary process. ③ To identify the importance of different drivers affecting ISA expansion at the local scale using the GWRF model, and to deeply elucidate the spatial heterogeneity characteristics among these drivers. Based on the above research objectives, this study establishes a systematic technical framework (Figure 1).

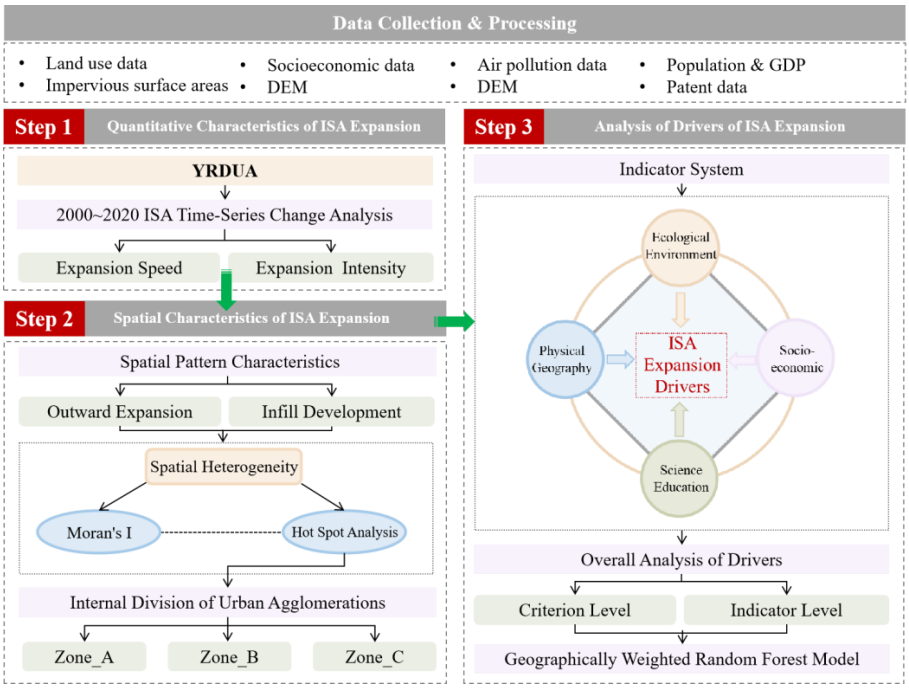

Figure 1. The technical roadmap.

2. Methodology

2.1. Overview of the Study Area

The YRDUA, located in the eastern coastal region of China, is the country's most economically developed and highly urbanized area (Figure 2). The ISAs in the YRDUA increased from 8.50% of the administrative area in 2000 to 30.36% in 2020, indicating a significant expansion trend. This expansion has not only exacerbated ecological and environmental pressures in urban and rural areas but also led to some degree of disorder in the region's spatial structure and land use patterns. Achieving sustainable urban and rural development while protecting the regional ecological environment amidst rapid urbanization has become a significant issue that urgently needs to be addressed in the YRDUA.

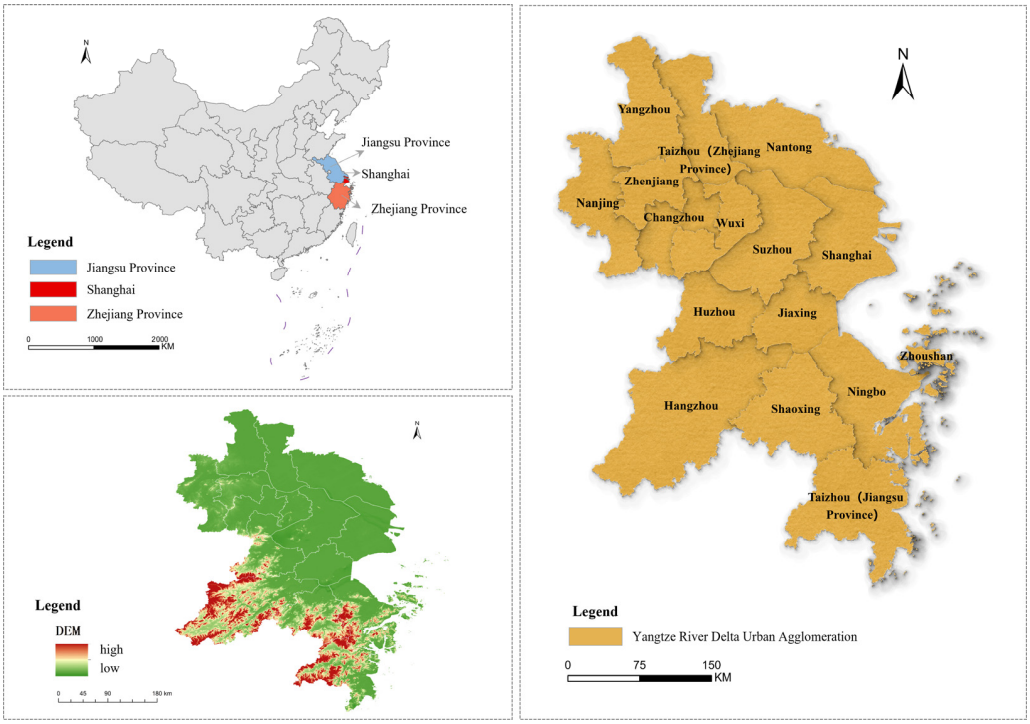

Figure 2. A location map of the Yangtze River Delta city cluster.

2.2. Data Sources and Processing

The data on ISAs were sourced from the Global Artificial Impervious Areas (GAIA) dataset, published by the team led by Peng Gong at Tsinghua University, and can be downloaded from http://data.ess.tsinghua.edu.cn (accessed on 28 November 2023). The spatial resolution is 30 m, with an overall accuracy of 90% [27]. The DEM was sourced from the Geospatial Data Cloud and can be downloaded from https://www.gscloud.cn (accessed on 12 March 2024). The administrative division data were sourced from the National Geoinformation Public Service Platform and can be downloaded from https://cloudcenter.tianditu.gov.cn/administrativeDivision (accessed on 11 November 2023). Statistical data were sourced from the statistical yearbooks of various cities and can be downloaded from the official government websites.

2.3. Research Methods

2.3.1. Spatial Expansion Characteristics of ISA

Expansion Dynamics Index

To quantify the ISA expansion dynamics, this study employed expansion speed (V) and intensity (R) metrics, capturing temporal and spatial characteristics of ISA growth. In

this study, the study period was divided into two intervals, T1 and T2, corresponding to 2000–2010 and 2010–2020, respectively. The formulas for calculation are as follows:

$$V_i = \frac{U_b - U_a}{T} \quad (1)$$

$$R_i = \frac{U_b - U_a}{U_a} \times \frac{1}{T} \times 100\% \quad (2)$$

V_i represents the expansion speed of ISAs in city i during the period, measured in $km^2 \cdot a^{-1}$; R_i represents the expansion intensity of ISA in city i during the period, measured in %; and U_a and U_b are the areas of ISAs at the beginning and end of the study period.

Moran's Index Method

Spatial autocorrelation can measure the degree of clustering of regional attribute values [35] and can visualize data to intuitively reflect the similarity of attribute values in adjacent units. In this study, the global Moran's I Index was used to explore the spatial dependence of ISAs in the study area, with specific calculation methods detailed in Rossi and Becker [36].

Hot Spot Analysis

Hot Spot Analysis can identify high-density and low-density areas where ISAs are clustered, thus providing a more comprehensive picture of the spatial distribution characteristics of ISAs. The Getis–Ord Gi* index was used to reveal the cold and hot spots of ISA expansion in the YRDUA, with specific calculation methods detailed in Rossi and Becker [36].

2.3.2. Analysis of ISA Expansion Drivers

Geographically Weighted Random Forest Model

The GWRF model is based on the concept of spatial variation coefficient models and consists of multiple local RF sub-models. It does not assume that data follow a Gaussian distribution [33]. The GWRF model serves as an effective tool for interpreting and predicting spatial heterogeneity and handling nonlinear relationships. The simplified expression of the traditional RF regression equation is given as follows [37]:

$$Yi = axi + e \quad (3)$$

where Yi is the dependent variable for the ith observation, axi is the RF nonlinear prediction based on a set of x independent variables, and e is the error term. Equation (3) is formed by inputting the entire dataset of variables without considering the spatial distribution characteristics of the variables.

The GWRF model incorporates the spatial location information of variables into the RF framework by fitting local RF sub-models to datasets of variables located in different spatial positions [37]. The equation is as follows:

$$Yi = a(ui, vi)xi + e \quad (4)$$

where a(ui, vi)xi is the prediction of the RF model calibrated at position i; and (ui, vi) are the coordinates of the spatial unit i.

Selection of ISA Expansion Drivers

To identify the drivers of ISA expansion, this study constructed a comprehensive indicator system based on an extensive literature review covering four guideline strata: ecological environment, physical geography, socio-economic, and science and education, as shown in Table 1.

Table 1. Indicators of drivers of ISA expansion in the YRDUA.

Criterion	Indicator	Notation	Unit
Ecological Environment	Green Cover Area in Urban Region	GCUR	ha
	Cultivated Land Area	CLA	1000 ha
	Industrial Sulphur Dioxide Emissions	ISDE	t
	Industrial Fume Removal	IFR	t
Physical Geography	Average Elevation	AE	m
	Average Slope	AS	
	Groundwater Resources	GR	10 m^3
Socio-economic	Population Density	PD	p/km^2
	GDP Growth Rate	GDPGR	%
	Number of Industrial Enterprises	NIE	No.
	Proportion of Primary Industry in GDP	PI	%
	Proportion of Secondary Industry in GDP	SI	%
	Area of City Paved Roads at Year-end	CPR	10,000 sq·m
	Residential Land Area	RL	km^2
Science and Education	Number of People in Scientific Research and Technological Services	NPSRT	No.
	Science and Technology Expenditure	STE	10,000 RMB
	Number of Patent Applications	PA	No.
	Number of People in Education	NPE	No.

Regarding the ecological environment, natural resources with high ecological value, such as green spaces and arable land, often limit ISA expansion in surrounding areas, which is crucial for sustainable urban development [38]. Rapid urbanization typically accompanies increased pollution, but effective environmental management measures can mitigate ISA expansion to some extent. Physical geography, topography, and hydrology directly constrain urban construction, affecting ISAs' spatial distribution. The average elevation and slope reflect surface undulation. Areas with significant topographical variation limit ISA formation and expansion, while plain areas favor it. Water resources and precipitation reflect hydrological conditions. Increased ISAs lead to higher runoff coefficients, causing urban issues and prompting decision-makers to adjust land use/cover layouts [39], consequently affecting the spatial distribution of ISAs. Socio-economically, rapid urban population and economic growth drive large-scale infrastructure development and urban land expansion, directly causing continuous ISA expansion [40]. Increased population density typically accelerates urbanization, exacerbating land use pressure and leading to ISA expansion [29]. GDP growth reflects economic development [40]. A higher proportion of secondary industries indicates a greater demand for production facilities, driving ISA expansion [41]. Furthermore, urbanization demands more land resources, particularly for residential and road areas, directly promoting ISA expansion [42].

However, scholars often overlook the role of science and education when studying the driving factors of urban ISA expansion. An increase in the number of educated individuals fosters the cultivation of scientific talents and enhances innovation capacity, promoting the application of new technologies in urban planning and construction, thus helping to reduce the expansion of ISAs. The increased expenditure on science and technology typically reflects investment in technological innovation. This can provide new technological solutions for urban management [43], thereby slowing the trend of increasing ISAs. Moreover, increased patent applications indicate higher innovative activity [44]. Innovations in environmental protection and urban construction can offer novel engineering and technological solutions to reduce ISAs.

3. Results and Analysis

3.1. Quantitative Characteristics of ISA Expansion

3.1.1. Overall Characteristics

From 2000 to 2020, the ISA expansion in the YRDUA increased significantly, growing from 9757.90 km^2 to 34,851.67 km^2, with a cumulative increase of 25,093.77 km^2. As shown in Figure 3, the YRDUA's ISAs have steadily increased yearly. However, when analyzing the annual increment of ISAs at yearly intervals, it is observed that from 2000 to 2016, despite fluctuations, there was an overall upward trend in the increment of ISAs. However, the new ISAs plummeted in the year after 2016 and have been on an overall downward trend since then.

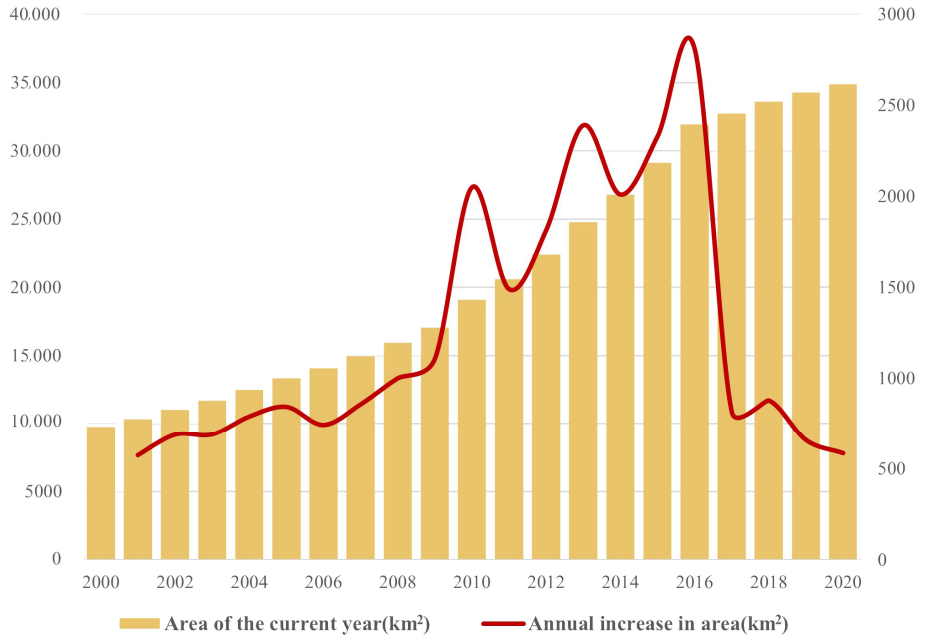

Figure 3. The year-to-year change in ISAs in the YRDAR from 2000 to 2020. The yellow bars show the total ISAs (km^2) each year, while the red line indicates the annual increase, highlighting periods of rapid growth and the subsequent slowdown after 2016.

From 2000 to 2020, the ISAs in various cities within the study area showed significant growth (Figure 4). Shanghai, Nantong, and Suzhou experienced the most rapid growth in ISAs, reflecting the accelerated urbanization process. In contrast, older major cities like Nanjing and Hangzhou had relatively lower growth rates due to their already high levels of urbanization in earlier years. Notably, even Zhoushan, which had the lowest ISAs, experienced nearly a fivefold increase over the past 20 years, indicating that the entire region is undergoing unprecedented urbanization.

3.1.2. Analysis of Expansion Speed and Intensity

The proportion of ISAs in the study area increased from 8.50% in 2000 to 30.36% in 2020. Additionally, the increase in ISAs during T1 and T2 accounted for 37.17% and 62.83% of the total new ISAs, respectively. It can be observed that the expansion area of ISAs during T2 is significantly larger than that during T1.

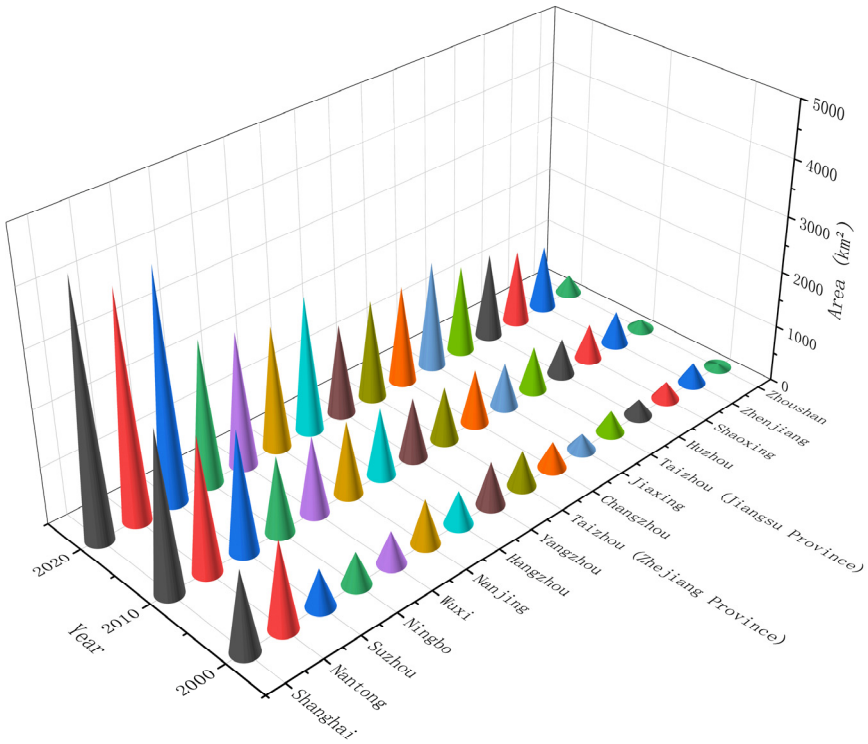

Figure 4. Changes in ISAs of cities in the YRDAR.

The expansion speed of ISAs during T1 and T2 was 932.63 km^2/a and 1576.75 km^2/a, respectively, while the expansion intensity was 9.56% and 8.26%. This indicates that although the expansion speed of ISAs during T2 was higher than that during T1, the expansion intensity was lower. This is because, by the beginning of the T2 period, there was already a significant amount of ISAs in the study area. Thus, despite the sizeable absolute increase, the base area of ISA was also large, resulting in lower expansion intensity. This trend reflects that land use in the YRDUA is moving towards a sustainable path. Although the growth intensity of ISAs has slowed, the absolute values remain high, warranting continuous attention.

3.2. Analysis of Spatial Heterogeneity of ISAs

3.2.1. Spatial Pattern Characteristics

As shown in Figures 5 and 6, by 2000, the initial growth nodes of ISAs had formed, although these nodes were relatively independent and did not yet demonstrate a trend of contiguous development. At this time, the growth nodes exhibited varying scales. During the T1 period, ISAs expanded outward from the growth nodes established in 2000, showing initial signs of contiguous development. By 2010, the outline of ISAs was largely established, leading to infill growth primarily within the contours formed by 2010 during the T2 period.

Specifically, the spatial distribution of ISAs in the YRDUA exhibits a pattern characterized by "strong in the east and weak in the west" and "one dominant area with multiple strong ones". Coastal mega-cities such as Shanghai, Nantong, and Suzhou, serving as economic hubs, have highly concentrated and rapidly growing ISAs, surpassing other cities to establish core area advantages. Simultaneously, several secondary aggregation centers have emerged with the rise of emerging cities like Jiaxing, Huzhou, and Taizhou. These peripheral growth poles around the core areas drive the gradual spread of ISAs across the YRDUA, transitioning from urban to rural areas and expanding from points to larger areas, blurring boundaries between cities and accelerating the formation of an integrated metropolitan spatial pattern.

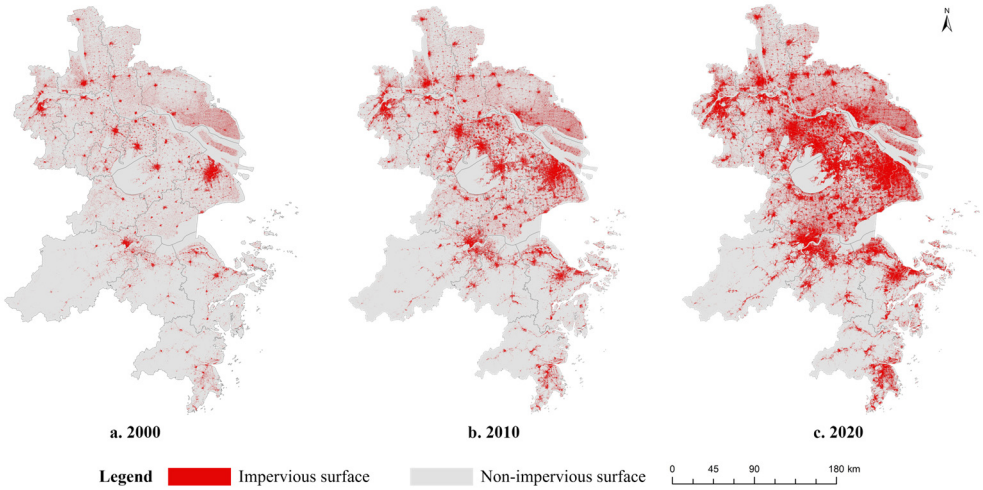

Figure 5. The spatial distribution of ISAs in the YRDUA for 2000 (**a**), 2010 (**b**), and 2020 (**c**).

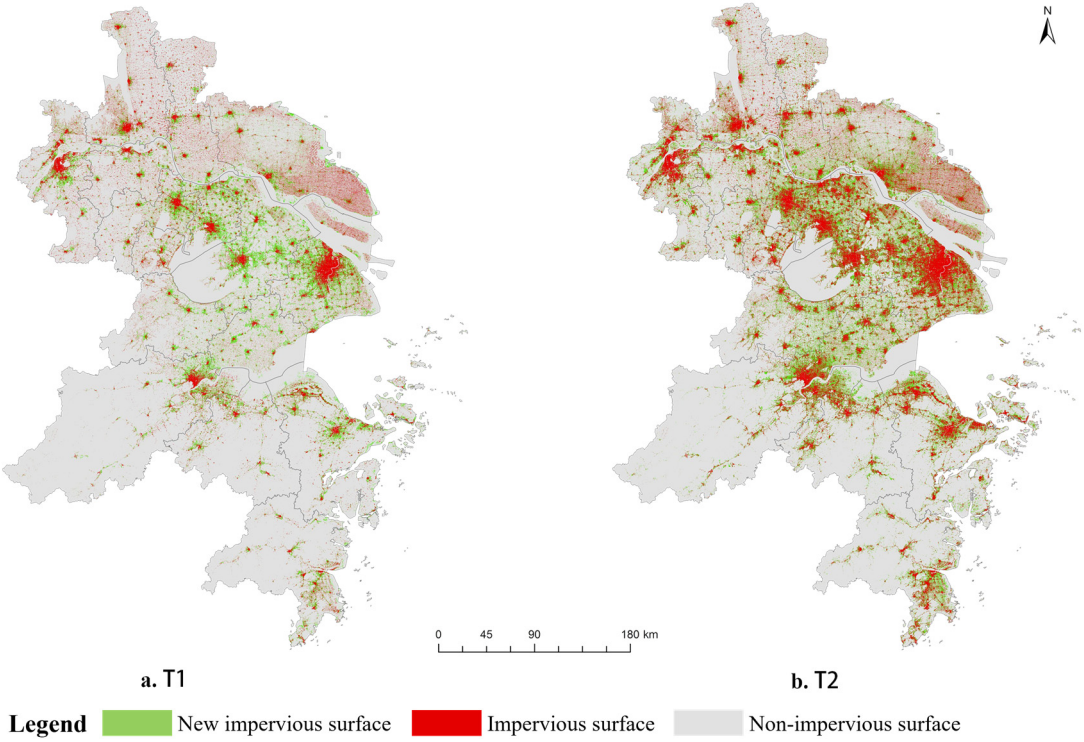

Figure 6. Changes in ISA spatial distribution in the YRDUA, highlighting new impervious surfaces (green) between T1 (**a**) and T2 (**b**).

3.2.2. Spatial Characteristics of ISA Expansion

Based on the spatial autocorrelation results, the global Moran's I index for ISA expansion in the YRDUA was 0.052 in 2000, 0.260 in 2010, and 0.326 in 2020. These values indicate that the expansion of ISAs in the YRDUA has exhibited spatial clustering characteristics over the past 20 years, with a trend towards further strengthening. As shown in Figure 7, the spatial clustering pattern and the spatiotemporal evolution of the ISAs in the YRDUA can be observed.

In 2000, the high-value clustering of ISAs in the region was primarily concentrated in economically developed coastal cities such as Shanghai, Nantong, Suzhou, and Taizhou. This formation included significant hotspots and secondary hotspots. Additionally, there were scattered cold spots, particularly in the southern part of Zhejiang province.

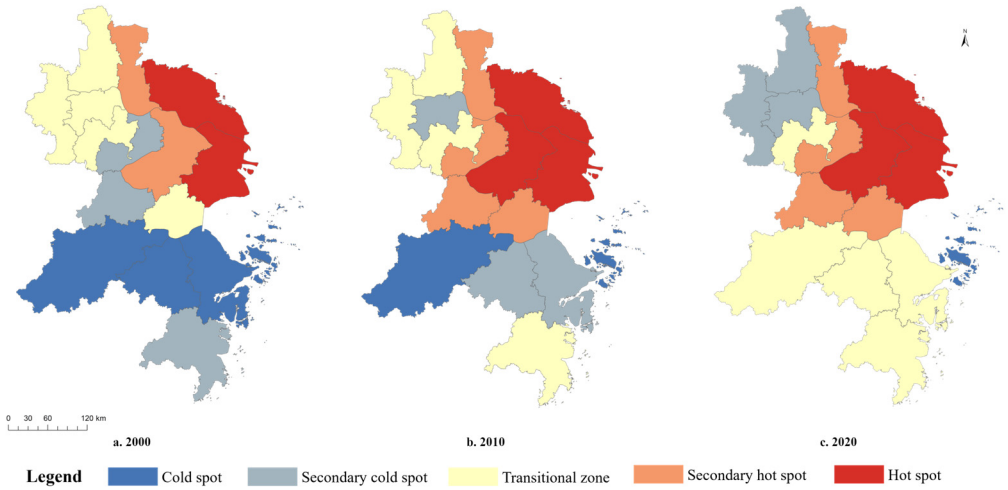

Figure 7. Results of the hotspot analysis of ISAs in the YRDUA for 2000 (**a**), 2010 (**b**), and 2020 (**c**).

In 2010, the hot spots and secondary hot spots of the ISAs further expanded in the region. All secondary hot spots were spatially adjacent to the hot spots, indicating that ISA expansion in the hot spots had a radiating effect on their surrounding areas. Additionally, the number of cold spots in the southern part of the YRDUA gradually decreased, transitioning into secondary cold spots and transitional zones, indicating that urbanization in the southern part of the YRDUA was accelerating.

In 2020, the range of hot spots and sub-hotspots remained the same as in 2010, indicating that the spatial pattern of the metropolitan area with Shanghai at its core has initially formed and stabilized. The southern part of the YRDUA is gradually transforming from cold spots and sub-cold spots into a transition zone, suggesting that the urbanization process in this region, while progressing, is still not as advanced as that of the core area of the YRDUA. At the same time, the areas of cold spots and sub-cold spots are gradually decreasing, reflecting the rapid increase in ISAs throughout the region.

According to the Hot Spot Analysis results, the YRDUA can be divided into three regions: "A-Development Decline Zone", "B-Development Core Zone", and "C-Development Ascendance Zone", as shown in Figure 8. Specifically, Zone A includes Nanjing, Yangzhou, Zhenjiang, and Changzhou; Zone B includes Taizhou, Nantong, Wuxi, Suzhou, Shanghai, Huzhou, and Jiaxing; and Zone C includes Hangzhou, Shaoxing, Ningbo, Zhoushan, and Taizhou. During the study period, Zone A was declining, transitioning from a transitional zone to a secondary cold spot. Zone B consistently remained in the hot spot or secondary hot spot category, gradually becoming the core area of the YRDUA over time. Zone C showed an ascending trend, transitioning from a cold spot to a transitional zone. Furthermore, it was observed that while ISA growth intensity in Zone C was lower than in Zone A in 2000, by 2020, it had surpassed that of Zone A. This indicates that urbanization efficiency in Zone C is significantly higher than in Zone A, suggesting that the comprehensive development potential of Zone C may be higher than that of Zone A.

3.3. Analysis of Drivers of ISA Expansion

3.3.1. Overall Analysis of Drivers

To ensure the scientific selection of indicators, a correlation test was conducted on the driving factors listed in Table 1 using a cor. test in R v.4.2.3 (http://www.r-project.org/, accessed on 16 October 2024) (Figure 9). All driving factors passed the collinearity test, with Pearson's R exceeding 0.8 [34] and the VIF remaining below 7.0 [45]. The reliability test results showed that Cronbach's $\alpha = 0.83$, indicating that the indicator system ensures the reliability of the measurement results for the driving factors of ISA expansion.

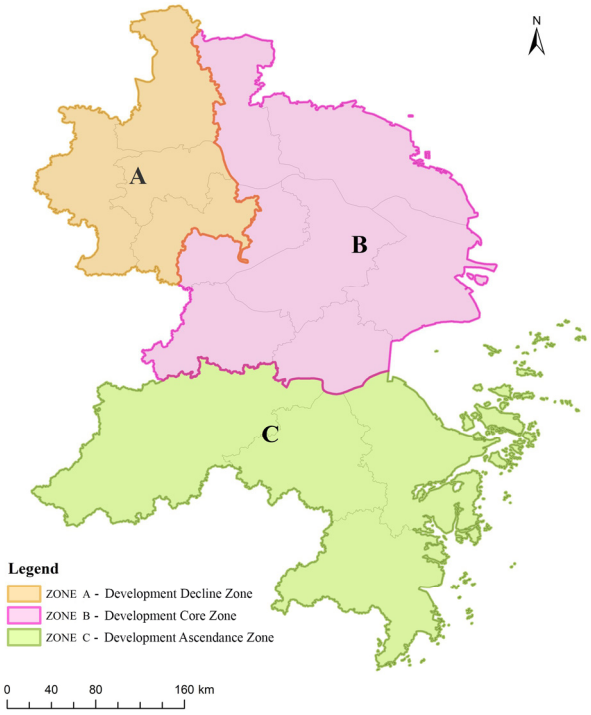

Figure 8. The YRDUA sub-region.

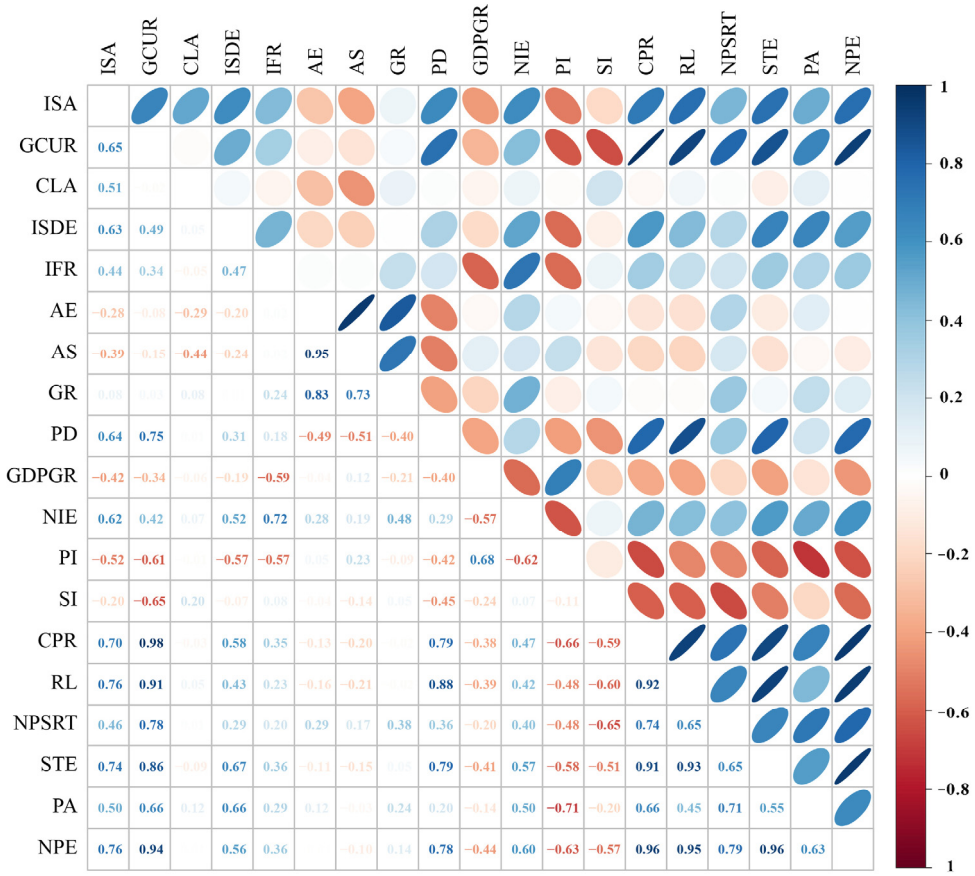

Figure 9. Pearson correlation coefficients for 18 influence factors.

From the criterion level (Figure 10), the importance of socio-economic factors consistently ranked first among the four criteria layers from 2000 to 2020. The scientific education

criteria also held a significant position, ranking second only to socio-economic factors. In 2000 and 2010, the importance of the ecological environment ranked third, while natural geographic criteria consistently ranked last. However, by 2020, the natural geographic criteria had risen from fourth to third place, while the ecological environment criteria had fallen to last place.

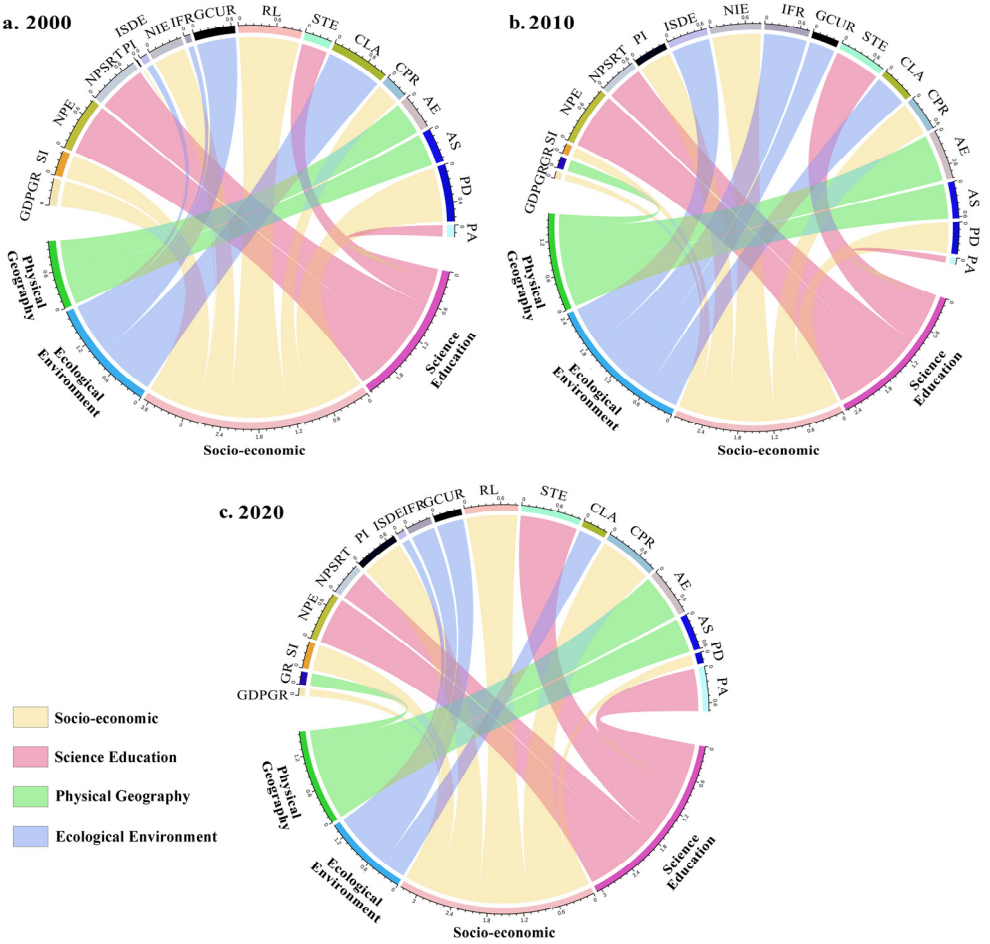

Figure 10. A comparison of the importance of guideline levels for drivers of ISAs in the YRDUA, (**a**) 2000, (**b**) 2010, (**c**) 2020.

From the indicator level (Figure 11), the five key factors influencing ISA expansion in 2000 were RL, PD, ETI, STI, and CLA. In 2010, the five key factors influencing ISA expansion were ETI, STE, AE, IFR, and NIE. In 2020, the five key factors influencing ISA expansion were CPR, STE, RL, AE, and ETI.

3.3.2. Spatial Heterogeneity of Drivers

In the GWRF model, an increase in error measures the change in overall model error by randomly shuffling feature values, demonstrating straightforwardly how features influence model performance under varying conditions. Using the natural break point method, the importance of driving factors was categorized into five levels: extremely high importance, high importance, medium importance, low importance, and extremely low importance. Darker colors indicate the higher importance of the driving factor for ISA expansion, while lighter colors indicate lower importance.

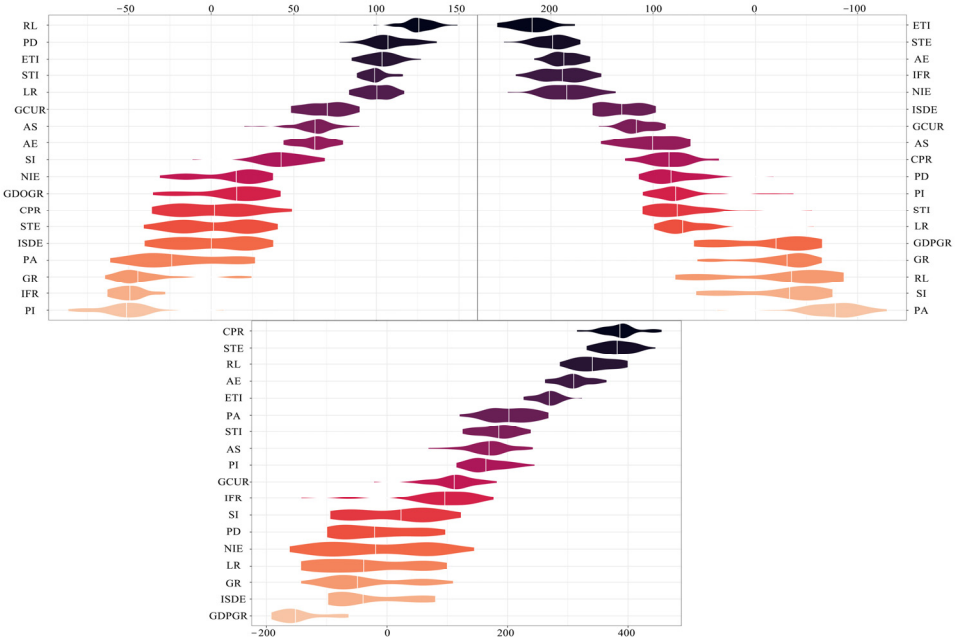

Figure 11. A comparison of the importance of drivers of ISA expansion in the YRDUA, 2000–2020.

Ecological Environment

As shown in Figure 12a. Areas with extremely high or high values of GCUR are primarily located in Zone B, with Shanghai consistently in the extremely high-value area. Areas with extremely low values influenced by GCUR shifted within Zone A and C, transitioning from Nanjing and Hangzhou to Changzhou and Ningbo. The impact of CLA shows an overall increasing trend in Zone A, while it remains relatively stable in Zone B; the area with extremely high values consistently falls within Nantong, reaching its peak in 2010. Areas with extremely low values were consistently in Shanghai for two consecutive periods. ISDE has a relatively balanced impact across the entire YRDUA, with minor variations among Zones A, B, and C. The impact of IFR shows an overall declining trend across Zones A, B, and C.

Physical Geography

As shown in Figure 12b. The areas with extremely high values of AE are concentrated in Zone B, notably with no occurrence of extremely high values in Zone A from 2000 to 2020. The areas with extremely low values influenced by AE have shifted from Taizhou, Suzhou, and Jiaxing to Taizhou and Jiaxing, later spreading to Yangzhou, with minimal changes in other zones. The variation in the influence of AS shows a pattern similar to the spatiotemporal distribution of AE from 2000 to 2010. The overall trend in the influence of GR shows a decline.

Socio-Economic

As shown in Figure 12c, the influence of PD shows a characteristic of initial diffusion followed by an overall decline, and by 2020, the influence of PD had decreased in Zones A, B, and C. The influence of GDPGR has increased overall, with the most significant increase in Zone C. In 2000, the areas with extremely high values expanded further within Zone C in 2010 and 2020. The influence of NIE initially decreased and then increased in different regions. The influence of the proportion of PI shows an overall declining trend in all three regions, particularly noticeable in Zone B. Similarly, the influence of CPR also decreased overall, with a concentration of areas with extremely low values in the western part. The influence of SI also decreased from 2000 to 2010, with areas of extremely high values shrinking from various regions to Zone B by 2010, while areas of extremely low

values expanded to Zone B; by 2020, the influence of SI had rebounded in various regions. The influence of RL continuously showed spatial heterogeneity in Zones A, B, and C.

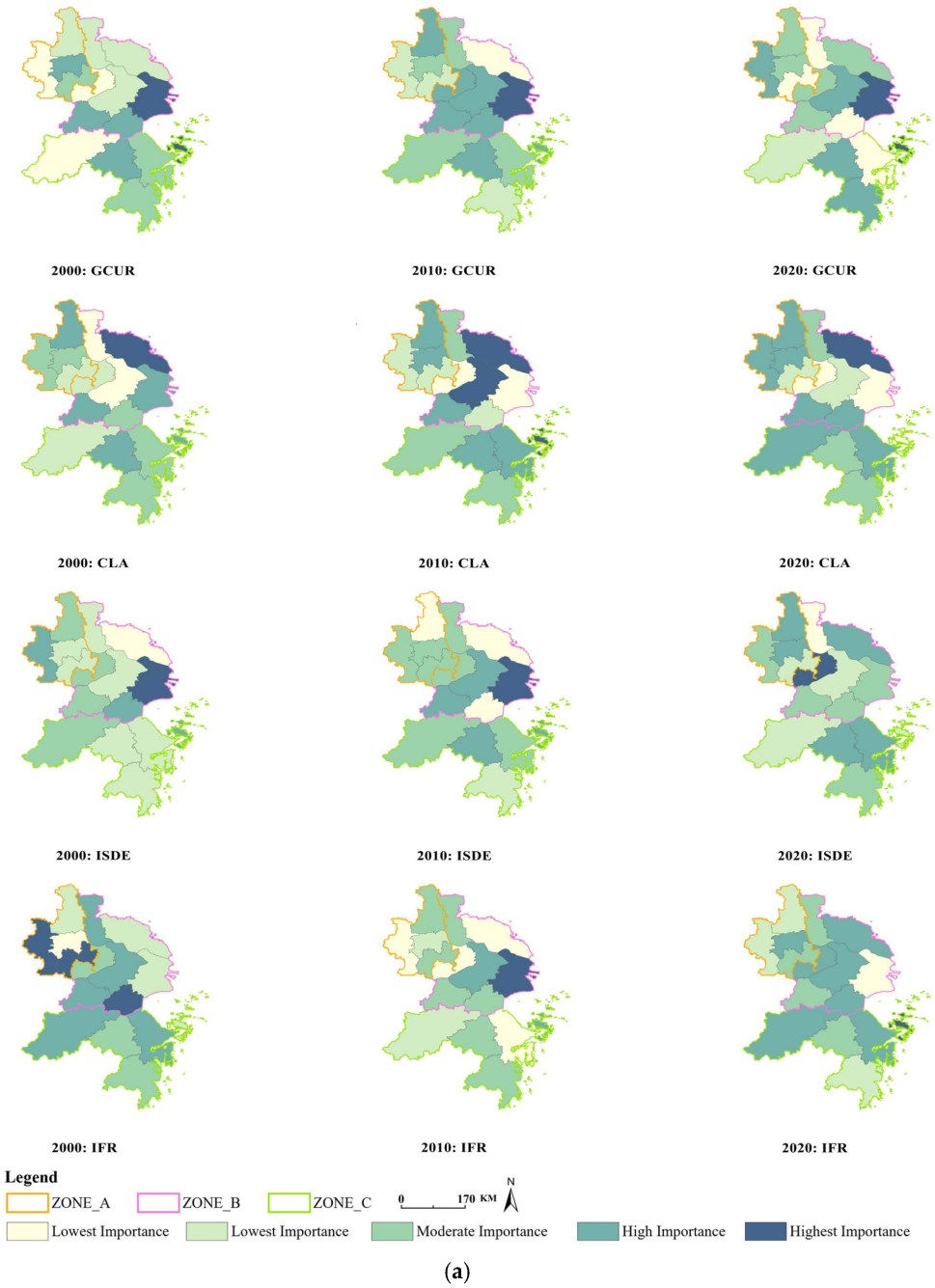

(**a**)

Figure 12. *Cont.*

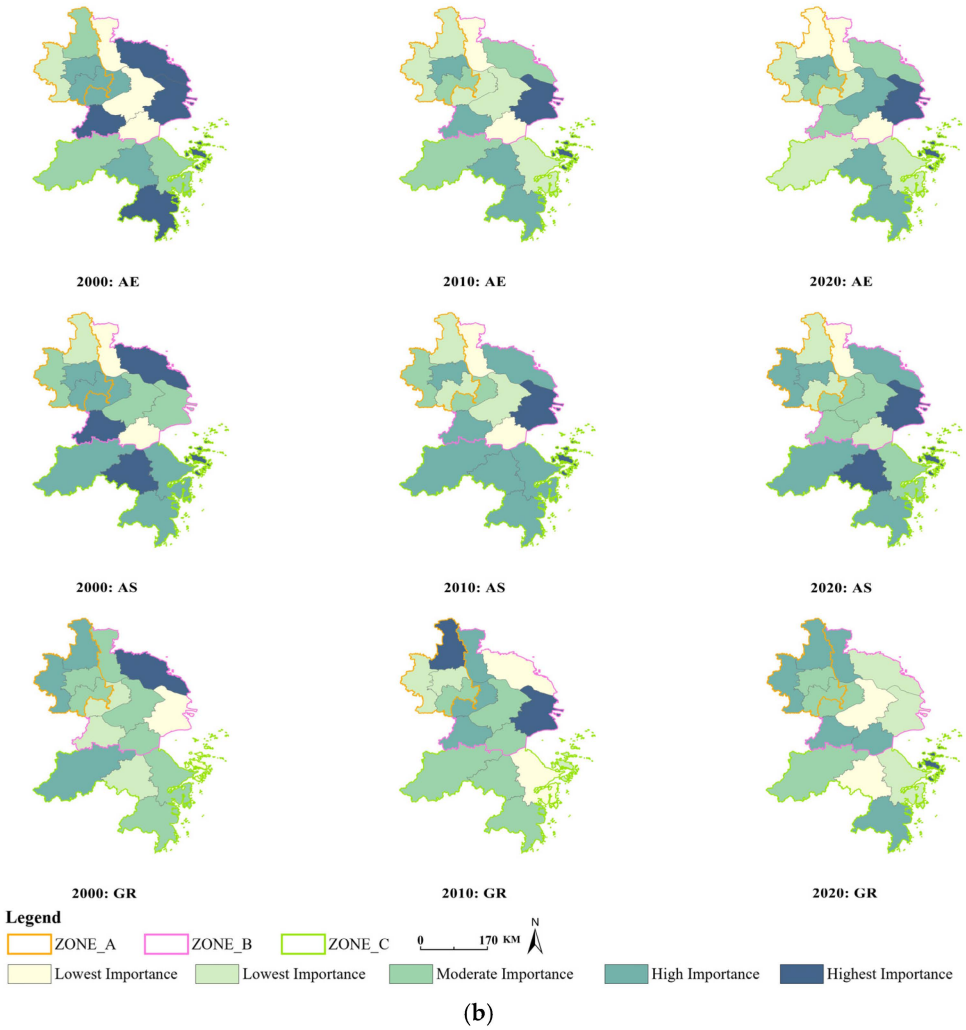

(**b**)

Figure 12. *Cont*.

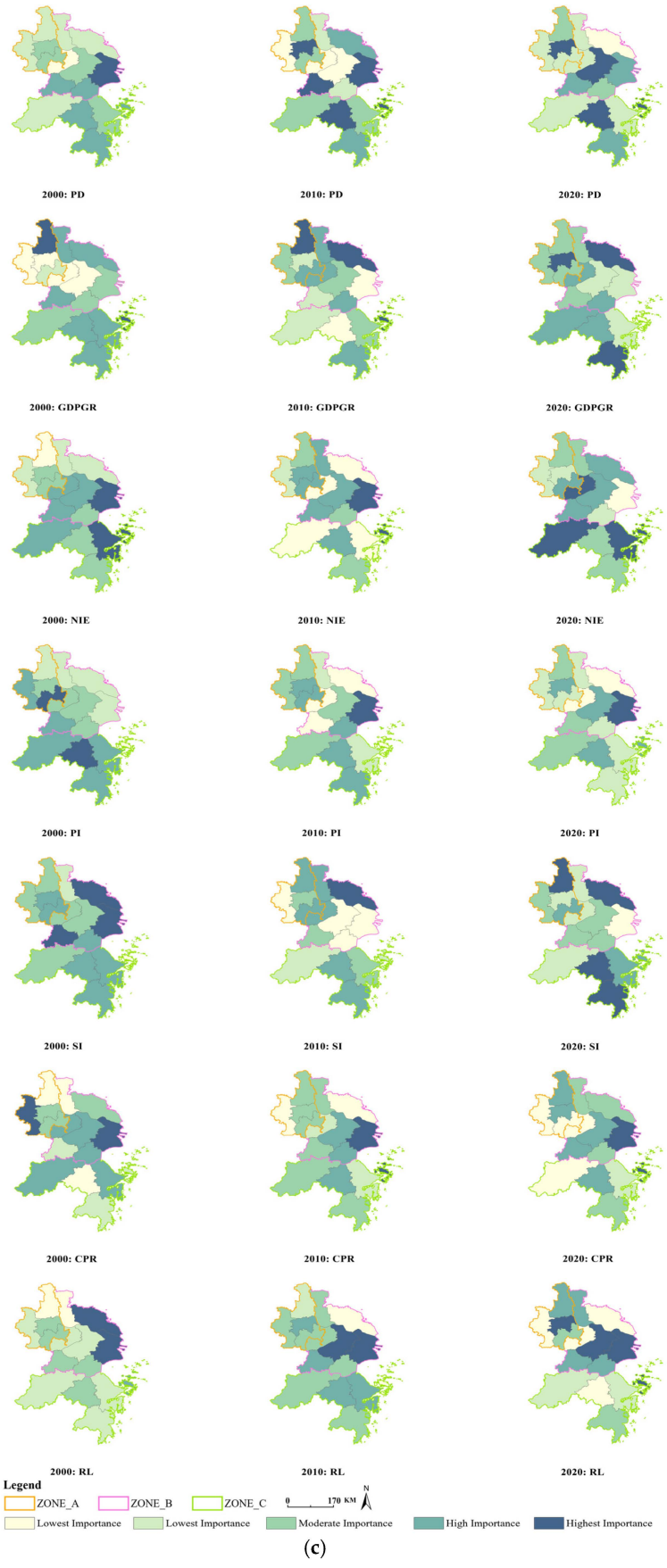

(**c**)

Figure 12. *Cont*.

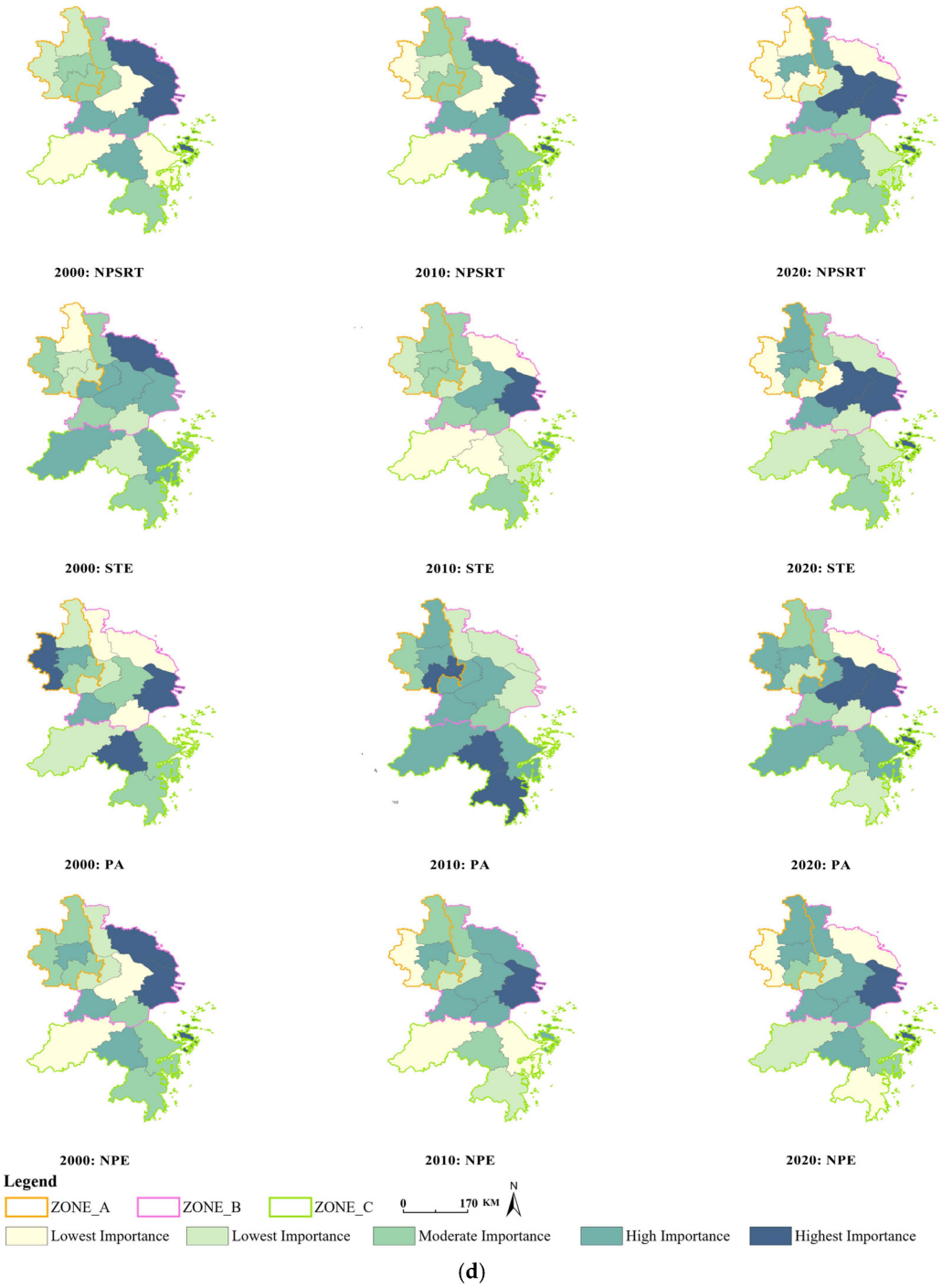

Figure 12. (**a**) The spatial and temporal distribution pattern of importance of ISA drivers in the YRDUA under the ecological guidelines layer, 2000–2020. (**b**) The pattern of spatial and temporal distribution of importance of ISA drivers in the YRDUA under the natural geography criterion layer, 2000–2020. (**c**) The spatial and temporal distribution patterns of importance of the drivers of ISAs in the YRDUA under the socio-economic layer, 2000–2020. (**d**) The spatial and temporal distribution patterns of importance of the drivers of ISAs in the YRDUA under the science education layer, 2000–2020.

Science and Education

As shown in Figure 12d. The areas with extremely high values of NPSRT have been consistently concentrated in Zone B from 2000 to 2020, with decreasing influence in Zone A and increasing influence in Zone C. The overall influence of STE shows a trend of initially

decreasing and then increasing. The influence of PA shows a pattern of initially increasing and then decreasing. Initially, areas with extremely high values were distributed in Zones A, B, and C, with relatively more areas of extremely low values in Zone B. By 2010, the influence of PA synchronously increased across the entire zone, followed by a decline by 2020. The influence of NPE shows a relatively higher impact in Zone B, with Shanghai consistently in the area of extremely high values. The variation in the influence of NPE in Zone A and C is relatively minor.

4. Discussion

This study reveals the continuous and rapid expansion trend of ISAs in the YRDUA from 2000 to 2020. This finding is consistent with previous research on the urbanization process in the YRDUA [46]. It is attributed to excessive local government support for real estate development, lax control over urban development boundaries, and imperfect regulations regarding the conversion of agricultural land to construction land. The rate of ISA expansion in the YRDUA has gradually slowed down, with urban expansion shifting from a "sprawl" to an "infill" pattern. This shift is influenced by increasing national emphasis on green development and ecological conservation [47]; local governments have become more cautious and efficient in using land and resources, avoiding the large-scale and disorderly expansion patterns seen in the past. However, there are spatial hierarchical differences in the clustering centers of ISAs in the YRDUA [48], which could potentially hinder the seamless integration of the metropolitan areas in the future. Therefore, enhancing regional cooperation will be essential to optimize spatial planning.

Previous studies using population data and nighttime light data [49] reveal that ISA distribution in the YRDUA is "strong in the east and weak in the west", forming a "dominant-single, multiple-strong, multi-center network". This study reaffirms these spatial differentiation patterns from the perspective of ISAs and further identifies that a few major cities like Shanghai have established absolute core area dominance. This study's key contribution lies in the in-depth analysis of the spatial and temporal evolution of ISAs expansion in the YRDUA, divided into three regions, and revealing a shift in the development center to the south. This finding challenges Zhen et al.'s conclusion of "strong in the east, weak in the west, and balanced in the north and south [50]" further enriching the understanding of urbanization in the area. Additionally, the division of this region breaks through administrative barriers, offering a new perspective for future macro-policy formulation for integrated regional development.

In addition, our findings reveal a relationship between industrial transformation and ISA expansion in the YRDUA. The significant impact of science and education factors on ISA expansion, particularly in Zones B and C, suggests a potential pathway for sustainable urban development. The historical expansion of ISAs since 2000 can be partially attributed to China's role as the 'world's factory' in the global economy [51]. However, the recent rise of knowledge-intensive and clean industries, supported by improved education levels, may help curb excessive ISA expansion [52]. This transformation highlights the potential of promoting education and clean industries as an effective strategy to balance economic growth with environmental protection.

Within the YRDUA, as a growth pole of the Chinese economy, scientific and technological innovation is the top priority for enhancing its competitiveness [53]. With improvements in education and technological innovation capabilities, the new generation of artificial intelligence technologies provides new tools for formulating sound development strategies [11]. These cities can utilize AI to create more scientific and reasonable urban planning, optimize traffic management, and develop smart cities, indirectly promoting efficient and intensive land use while curbing the uncontrolled growth of ISAs [54].

Although government and public attention to ecological protection has increased in recent years [55], overall, ISAs continue to rise. The government should further strengthen ecological policies and fully leverage new information technologies in urban governance to build a more scientific and efficient planning system while promoting comprehensive,

green, and low-carbon development. It should also focus on the guiding role of planning, formulate urban and land use plans scientifically, set reasonable urban development boundaries, and strictly control development intensity [56]. To effectively implement these policy measures, differentiated development strategies should be formulated based on the distinct characteristics and needs of different regions. For Zone A, we recommend urban regeneration strategies focusing on existing ISA renovation and smart city technologies to improve land-use efficiency [57]. For Zone B, where ecological factors show persistent importance, priorities should focus on integrating blue–green infrastructure with ISAs to enhance urban resilience while maintaining its core position. For Zone C, which demonstrates high development potential, we propose a "leap-forward smart growth" strategy, combining transit-oriented development principles with ecological preservation to guide rational ISA expansion. These targeted recommendations aim to promote coordinated regional development while respecting the spatial heterogeneity revealed by our analysis.

This study introduces several methodological innovations. Using hotspot analysis, the YRDUA was classified into the "Development Decline Zone", "Development Core Zone", and "Development Ascendance Zone", highlighting regional development trends to inform coordinated policies. While the methodology was tailored specifically for the YRDUA, it holds potential for application in other urban agglomerations with similar characteristics. The combination of ISAs with specific spatial and statistical methods offers a framework to identify urban expansion patterns, providing a model that may be adapted to other regions. It also uniquely incorporates scientific education as a driving factor and applies the GWRF model, capturing nonlinear relationships and enhancing explanatory power. However, limitations exist. The study lacks urban 3D pattern data (e.g., building height and type), which could better characterize urban sprawl. Additionally, its macro-level approach may overlook city-specific policy and economic variations. Future research could address these gaps through 3D data and case studies to better understand ISA expansion drivers.

5. Conclusions

Regarding spatiotemporal pattern characteristics, the ISAs have evolved from a point distribution to a regionally clustered form, forming a spatial pattern of "one dominant area with multiple strong ones". Temporally, the expansion of ISAs can be divided into two stages: an initial phase characterized by outward expansion from growth nodes and a later phase dominated by infill development. Based on the expansion patterns of ISAs, the YRDUA can be divided into three regions: the "A-Development Decline Zone", "B-Development Core Zone", and "C-Development Ascendance Zone". Zone B represents the core area of the YRDUA, while Zone C has higher overall development potential compared to Zone A. Regarding the drivers, there was significant spatial heterogeneity in the importance of different drivers for ISA expansion. Ecological environment factors such as GCUR and CLA maintained importance in Zone B. Physical geography factors, particularly AE, were concentrated in Zone B. Socio-economic drivers like PD, initially significant in Zone B, gradually spread to Zones A and C. The GDP growth rate gained prominence in parts of Zones A and C. In terms of science and education factors, NPSRT had the greatest impact in Zone B, while the importance of STE increased beyond its initial concentration in Zone B, extending to parts of Zone C.

Author Contributions: Conceptualization, B.Z. and X.J.; methodology, Y.W.; software, B.Z. and Y.W.; investigation, H.G. and X.J.; writing—original draft preparation, B.Z. and Y.W.; writing—review and editing, B.Z. and Y.W.; visualization, B.Z. and Y.W.; supervision, L.L.; project administration, H.G. All authors have read and agreed to the published version of the manuscript.

Funding: This research received no external funding.

Data Availability Statement: The raw data supporting the conclusions of this article will be made available by the authors on request.

Conflicts of Interest: The authors declare no conflicts of interest.

References

1. He, J.; Zhang, Y.; Li, X.; Liu, H. Measuring urban spatial interaction in Wuhan Urban Agglomeration, Central China: A spatially explicit approach. *Sustain. Cities Soc.* **2017**, *32*, 569–583. [CrossRef]
2. Touchaei, A.G.; Akbari, H.; Tessum, C.W. Effect of increasing urban albedo on meteorology and air quality of Montreal (Canada)—Episodic simulation of heat wave in 2005. *Atmos. Environ.* **2016**, *132*, 188–206. [CrossRef]
3. Morabito, M.; Kuehler, R.; Lopez, A. Surface urban heat islands in Italian metropolitan cities: Tree cover and impervious surface influences. *Sci. Total Environ.* **2021**, *751*, 142334. [CrossRef] [PubMed]
4. Ye, C.; Liu, Z.; Zhang, W. Assessment and analysis of regional economic collaborative development within an urban agglomeration: Yangtze River Delta as a case study. *Habitat Int.* **2019**, *83*, 20–29. [CrossRef]
5. National Bureau of Statistics of China. *Statistical Communiqué of the People's Republic of China on the 2023 National Economic and Social Development*; National Bureau of Statistics of China: Beijing, China, 2023.
6. Li, Z.; Sun, Z.; Tian, Y.; Zhong, J.; Yang, W. Impact of Land Use/Cover Change on Yangtze River Delta Urban Agglomeration Ecosystem Services Value: Temporal-Spatial Patterns and Cold/Hot Spots Ecosystem Services Value Change Brought by Urbanization. *Int. J. Environ. Res. Public Health* **2019**, *16*, 123. [CrossRef] [PubMed]
7. Slonecker, E.T.; Jennings, D.B.; Garofalo, D. Remote sensing of impervious surfaces: A review. *Remote Sens. Rev.* **2001**, *20*, 227–255. [CrossRef]
8. Zhang, C.; Wu, W.; Xu, B. An object-based convolutional neural network (OCNN) for urban land use classification. *Remote Sens. Environ.* **2018**, *216*, 57–70. [CrossRef]
9. Yin, R.; Liu, Y.; Zhang, L.; Li, X. Automatic framework of mapping impervious surface growth with long-term Landsat imagery based on a temporal deep learning model. *IEEE Geosci. Remote Sens. Lett.* **2021**, *19*, 1–5. [CrossRef]
10. Deng, C.; Zhu, Z. Continuous subpixel monitoring of urban impervious surface using Landsat time series. *Remote Sens. Environ.* **2020**, *238*, 110929. [CrossRef]
11. Mahyoub, S.; Al-Muhtadi, J.; Al-Hadhrami, S. Impervious surface prediction in Marrakech city using artificial neural network. *Int. J. Adv. Comput. Sci. Appl.* **2022**, *13*, 183–189. [CrossRef]
12. Tang, Y.; Li, X.; Zhang, L. Mapping impervious surface areas using time-series nighttime light and MODIS imagery. *Remote Sens.* **2021**, *13*, 1900. [CrossRef]
13. Shuster, W.D.; Bonta, J.; Thurston, H.W.; Warnemuende, E.; Smith, B. Impacts of impervious surface on watershed hydrology: A review. *Urban Water J.* **2005**, *2*, 263–275. [CrossRef]
14. Yang, X.; Liu, Z. Use of satellite-derived landscape imperviousness index to characterize urban spatial growth. *Comput. Environ. Urban Syst.* **2005**, *29*, 524–540. [CrossRef]
15. Zhao, C.; Li, J.; Wang, X.; Zhang, Y. Analysis of changes in the spatiotemporal characteristics of impervious surfaces and their influencing factors in the Central Plains Urban Agglomeration of China from 2000 to 2018. *Heliyon* **2023**, *9*, e18849. [CrossRef]
16. Jian, P.; Zhang, Y.; Yang, Y. Using impervious surfaces to detect urban expansion in Beijing of China in the 2000s. *Chin. Geogr. Sci.* **2016**, *26*, 229–243. [CrossRef]
17. Liu, F.; Zhang, L.; Chen, Y. Impervious surface expansion: A key indicator for environment and urban agglomeration—A case study of Guangdong-Hong Kong-Macao Greater Bay Area using Landsat data. *J. Sens.* **2020**, *2020*, 3896589. [CrossRef]
18. Liu, Y.; Cakmak, S.; Peters, P. Comparison of land use regression and random forests models on estimating noise levels in five Canadian cities. *Environ. Pollut.* **2020**, *256*, 113367. [CrossRef]
19. Wu, M.; Zhang, L.; Wang, J. A hierarchical multiscale super-pixel-based classification method for extracting urban impervious surfaces using deep residual networks from WorldView-2 and LiDAR data. *IEEE J. Sel. Top. Appl. Earth Obs. Remote Sens.* **2019**, *12*, 210–222. [CrossRef]
20. Li, M.; Zang, S.; Wu, C.; Na, X. Spatial and temporal variation of the urban impervious surface and its driving forces in the central city of Harbin. *J. Geogr. Sci.* **2018**, *28*, 323–336. [CrossRef]
21. Gao, C.; Li, X.; Wang, Y. 50-year urban expansion patterns in Shanghai: Analysis using impervious surface data and simulation models. *Land* **2023**, *12*, 2065. [CrossRef]
22. Cao, X.; Li, Y.; Zhang, H. Expansion of urban impervious surfaces in Xining city based on GEE and Landsat time series data. *IEEE Access* **2020**, *8*, 147097–147111. [CrossRef]
23. Zhou, Z.L.; Chen, X.L.; Li, J.M. Temporal and spatial variations of impervious surface landscape pattern and the driving factors in Xiamen City, China. *J. Appl. Ecol.* **2020**, *31*, 230–238. [CrossRef]
24. Lu, S.; Guan, X.; He, C.; Zhang, J. Spatio-Temporal Patterns and Policy Implications of Urban Land Expansion in Metropolitan Areas: A Case Study of Wuhan Urban Agglomeration, Central China. *Sustainability* **2014**, *6*, 4723–4748. [CrossRef]
25. Ma, Q.; Wu, J.; Wang, Y. Spatial scaling of urban impervious surfaces across evolving landscapes: From cities to urban regions. *Landsc. Urban Plan.* **2018**, *175*, 50–61. [CrossRef]
26. Zhu, H.; Ou, X.; Yang, Z.; Yang, Y.; Ren, H.; Tang, L. Spatiotemporal Dynamics and Driving Forces of Land Urbanization in the Yangtze River Delta Urban Agglomeration. *Land* **2022**, *11*, 1365. [CrossRef]
27. Li, X.; Liu, K.; Tian, S.; Zhang, J. Evaluation of urban human settlements resilience based on the DPSIR model: A case study of the Yangtze River Delta urban systems. *Hum. Geogr.* **2022**, *37*, 54–62. [CrossRef]
28. Wang, Y.; Kang, L.Y.; Wu, X.Q.; Zhang, J. Estimating the environmental Kuznets curve for ecological footprint at the global level: A spatial econometric approach. *Ecol. Indic.* **2013**, *34*, 15–21. [CrossRef]

29. Wu, W.; Li, X.; Zhang, Y.; Liu, J. Change of impervious surface area and its impacts on urban landscape: An example of Shenyang between 2010 and 2017. *Ecosyst. Health Sustain.* **2020**, *6*, 1767511. [CrossRef]
30. Wu, X.; Yang, S.; Yin, S.; Xu, H. Spatial-temporal dynamic characteristics and its driving mechanism of urban built-up area in Yangtze River Delta based on GTWR model. *Resour. Environ. Yangtze Basin* **2021**, *30*, 2594–2606.
31. Brokamp, C.; He, X.; Huang, Y. Exposure assessment models for elemental components of particulate matter in an urban environment: A comparison of regression and random forest approaches. *Atmos. Environ.* **2017**, *151*, 1–11. [CrossRef]
32. Nilsson, P. Natural amenities in urban space—A geographically weighted regression approach. *Landsc. Urban Plan.* **2014**, *121*, 45–54. [CrossRef]
33. Grekousis, G.; Feng, Z.; Marakakis, I.; Lu, Y.; Wang, R. Ranking the importance of demographic, socioeconomic, and underlying health factors on US COVID-19 deaths: A geographical random forest approach. *Health Place* **2022**, *74*, 102744. [CrossRef] [PubMed]
34. Zhao, H.; Gu, T.; Sun, D.; Miao, C. Dynamic evolution and influencing mechanism of urban human settlements in the Yellow River Basin from the perspective of "production-living-ecological" function. *Acta Geogr. Sin.* **2023**, *78*, 2973–2999. [CrossRef]
35. Anselin, L. Local indicators of spatial association—LISA. *Geogr. Anal.* **1995**, *27*, 93–115. [CrossRef]
36. Rossi, F.; Becker, G. Creating forest management units with Hot Spot Analysis (Getis-Ord Gi*) over a forest affected by mixed-severity fires. *Aust. For.* **2019**, *82*, 166–175. [CrossRef]
37. Georganos, S.; Grippa, T.; Niang Gadiaga, A.; Linard, C.; Lennert, M.; Vanhuysse, S.; Mboga, N.; Wolff, E.; Kalogirou, S. Geographical random forests: A spatial extension of the random forest algorithm to address spatial heterogeneity in remote sensing and population modelling. *Geocarto Int.* **2019**, *36*, 121–136. [CrossRef]
38. Santhanam, H.; Majumdar, R. Quantification of green-blue ratios, impervious surface area, and pace of urbanisation for sustainable management of urban lake–land zones in India: A case study from Bengaluru city. *J. Urban Manag.* **2022**, *11*, 310–320. [CrossRef]
39. Liang, Z.; Zhao, Y.; Fu, Y. Optimization of spatial pattern of urban imperviousness based on the integration of SCS-CN hydrological model and the ant colony algorithm. *J. Geo-Inf. Sci.* **2017**, *19*, 1315–1326. [CrossRef]
40. Meng, L.; Si, W. The driving mechanism of urban land expansion from 2005 to 2018: The case of Yangzhou, China. *Int. J. Environ. Res. Public Health* **2022**, *19*, 15821. [CrossRef]
41. Yan, D.; Yang, J. Change in spatial distribution of population and economy and influencing factors in the Yangtze River Delta. *Prog. Geogr.* **2017**, *36*, 820–831. [CrossRef]
42. Long, F.; Zheng, L.; Song, Z. High-speed rail and urban expansion: An empirical study using a time series of nighttime light satellite data in China. *J. Transp. Geogr.* **2018**, *72*, 106–118. [CrossRef]
43. Song, M.; Wang, S.; Wu, K. Environment-biased technological progress and industrial land-use efficiency in China's new normal. *Ann. Oper. Res.* **2018**, *268*, 425–440. [CrossRef]
44. Barrichello, A.; dos Santos, E.G.; Morano, R.S. Determinant and priority factors of innovation for the development of nations. *Innov. Manag. Rev.* **2020**, *17*, 307–320. [CrossRef]
45. Tian, Y.; Mao, Q. The effect of regional integration on urban sprawl in urban agglomeration areas: A case study of the Yangtze River Delta, China. *Habitat Int.* **2022**, *130*, 102695. [CrossRef]
46. Meng, L.; Sun, Y.; Zhao, S. Comparing the spatial and temporal dynamics of urban expansion in Guangzhou and Shenzhen from 1975 to 2015: A case study of pioneer cities in China's rapid urbanization. *Land Use Policy* **2020**, *97*, 104753. [CrossRef]
47. Sun, B.; Hua, J.; Li, W.; Zhang, T. Spatial structure change and influencing factors of city clusters in China:From monocentric to polycentric based on population distribution. *Prog. Geogr.* **2017**, *36*, 1294–1303. [CrossRef]
48. Yu, M.; Zhang, M.; Xu, H.; Liu, Y.; Zhou, Y. Spatiotemporal heterogeneity analysis of Yangtze River Delta urban agglomeration: Evidence from nighttime light data (2001–2019). *Remote Sens.* **2021**, *13*, 1235. [CrossRef]
49. Sun, J.; Zhou, X. Spatial structure and influencing factors of the Yangtze River Delta urban agglomeration from a multidimensional perspective: Based on NPP-VIIRS nighttime light data and Gaode's population migration data. *Econ. Geogr.* **2023**, *43*, 78–88. [CrossRef]
50. Zhen, M.; Dang, A.; Kan, C. Study on the Identification of Urban Agglomerations in the Yangtze River Delta Based on Big Data and Network Analysis. *Shanghai Urban Plan. Rev.* **2019**, *6*, 8–16.
51. Zhang, K.M.; Wen, Z.G. Review and challenges of policies of environmental protection and sustainable development in China. *J. Environ. Manag.* **2008**, *88*, 1249–1261. [CrossRef]
52. Zhang, J.; Li, S. The Impact of Human Capital on Green Technology Innovation-Moderating Role of Environmental Regulations. *Int. J. Environ. Res. Public Health* **2023**, *20*, 4803. [CrossRef] [PubMed]
53. Kandt, J.; Batty, M. Smart cities, big data and urban policy: Towards urban analytics for the long run. *Cities* **2021**, *109*, 102992. [CrossRef]
54. Luo, X.; Cheng, C.; Pan, Y.; Yang, T. Coupling coordination and influencing factors of land development intensity and urban resilience of the Yangtze River Delta urban agglomeration. *Water* **2022**, *14*, 1083. [CrossRef]
55. Engin, Z.; van Dijk, J.; Lan, T.; Longley, P.A.; Treleaven, P.; Batty, M.; Penn, A. Data-driven urban management: Mapping the landscape. *J. Urban Manag.* **2020**, *9*, 140–150. [CrossRef]

56. Sun, F.; Liu, M.; Wang, Y.; Wang, H.; Che, Y. The effects of 3D architectural patterns on the urban surface temperature at a neighborhood scale: Relative contributions and marginal effects. *J. Clean. Prod.* **2020**, *258*, 120706. [CrossRef]
57. Zhu, Y.; Song, J.; Bai, Y. China's Urban Regeneration Evolution from 1949 to 2022: From the Perspective of Governance Mode. *Land* **2024**, *13*, 1806. [CrossRef]